

An Innovative Solution for Suburban Railroad Transportation: The Gas Turbine-Hybrid Train

R. Capata*, E. Sciubba

Dept. of Mechanical and Aeronautical Engineering
University of Roma I "La Sapienza" Roma, Italy
Tel. +390644585271; Fax: +39064881749
E-mail: roberto.capata@uniroma1.it

Abstract

The paper reports the latest results of a study conducted on a hybrid train in which a gas turbine, operating in several alternative control modes (fixed point, on-off or load-following), generates the electrical energy for recharging a battery package and for driving the electric motors of a suburban train. The model, originally developed for automotive applications, has been validated by experimental tests performed on an ELLIOTT TA-45 GT group in the ENEA-Casaccia Research Center.

This paper describes the preliminary design of the traction system and the choice of the energy flow control strategy. Numerical simulations have been carried out, based on an actual train mission (the Norwegian railroad track between Asker and Lillehammer) and on industrial data for the single components. Following two different approaches, separate optimizations of the gas turbine set and battery package are performed, in which the objective function is the monetary cost per mission or, which is equivalent, the kWh/(t-km) for a given mission profile.

Keywords: GT-driven hybrid propulsion, railroad transportation systems, transportation costs

1. General Overview

The train object of the present study is composed of four railroad coaches for a total length of 85 m, a width of 3.10 m, a height of 4.125 m and 197 t of gross weight. Its all-electric version is presently in service on Norwegian railroads, with a certified maximum speed of 160 km/h and a maximum acceleration of 0.85 m/s²; its shape is quite similar to the Diesel IC4 train shown in Figure 1 (recently purchased by the Danish State Railways from AnsaldoBreda). The convoy is equipped with four electric motors, for a total net power of 2.8 MW.

1.1 Description of the GT-based hybrid system

As described in (AnsaldoBreda, 2001), the GT-hybrid propulsion system proposed here consists of a gas turbine set (Figure 2) driving an electrical AC/DC inverter. The generator output is managed by a Vehicle Management Unit (VMU) that - working under a logic to be discussed below - satisfies the instantaneous power demand by means of electric motors (M). A properly sized battery pack serves as an energy

buffer, and is recharged by excess power and by electrical braking energy recovery. The GT set can be operated at fixed point or in a *load following* (in a sense discussed below) mode; in this latter case, the gas turbine runs at constant speed, and its power output is varied by controlling both the geometry (IGV on the compressor and VIGV on the turbine) and the fuel flow rate.



Figure 1. The IC4 Diesel train

*Author to whom correspondence should be addressed

In this paper, the *degree of hybridization* of a certain configuration is defined as the ratio of the installed electrical power of the gas turbine to the total installed net power:

$$I_{hyb} = P_{GT} / (P_{GT} + P_{BAT}) \quad (1)$$

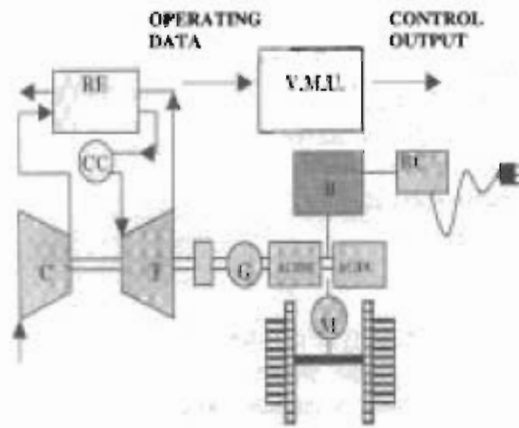


Figure 2. GT Hybrid Series transmission scheme

1.2 Design data

The assigned design specifications are:

$r = 0.5 \text{ m}$	rolling radius of the train wheels
$m = 197 \text{ t}$	train overall weight
$\alpha = 0$	slope of the track
$b = 3.1 \text{ m}$	overall train width
$h = 4.250 \text{ m}$	overall train height
$f = 0.005$	wheel-railtrack friction coefficient
$c_x = 0.45$	aerodynamic drag coefficient
$\eta_{gen} = 0.8$	electric generator efficiency
$\eta_{trans} = 0.8$	transmission efficiency
$P_{sp} = 150 \text{ W/kg}$	Pb-acid batteries specific power
$E_{sp} = 35 \text{ Wh/kg}$	Pb-acid batteries specific energy

These data - together with a specified mission schedule - are used to calculate the instantaneous power required at the wheels (Figures 4, 5). The details of the calculations are omitted here, and interested readers are referred to (Capata and Sciubba, 2002, Capata et al., 2003, Cioffarelli, 2004).

2. The Logic of the Simulation

The design goal was to identify the *optimal* configuration as the one that would attain the minimal yearly operational costs. Since these costs depend on the fuel consumption per mission and by the installed GT and B powers, it is clear that the "optimization" presented here is strictly valid only for the assigned mission path (Lillehammer-Asker in this case). A different path would in fact in all likelihood modify the instantaneous power requirement, thus influencing the fuel consumption and the values of installed

power. This leads to a major drawback: if the mission is changed, both the optimal configuration and the optimal control strategy may vary. In fact, we have compared the effects of different types of control logic on the overall mission performance for a single assigned instantaneous power demand curve. The logic is represented by the flow charts of Figures 3, 4 and 5.

- a) If the instantaneous net power supplied by the GT group is larger than the instantaneous power demand, then the electric generator M exceeds the energy request and the energy surplus is directed to the battery:

$$\begin{aligned} \text{IF } P_{GT} > P_{train} \quad \text{THEN} \\ P_M = P_{train} \Rightarrow \\ P_{bat} = P_{GT} - P_{train} \end{aligned} \quad (2)$$

- b) If, on the opposite, the instantaneous net GT power is lower than the train demand, the total required instantaneous power is jointly provided by the battery and GT.

$$\begin{aligned} \text{IF } P_{GT} < P_{train} \quad \text{THEN} \\ P_M = P_{GT} + P_{bat} \end{aligned} \quad (3)$$

The constraints introduced in the numerical procedure are the following:

- The energy flows must *close the balance* at each instant in time ($\Delta E_{tot} = 0$);
- The battery SOC is allowed to vary only between a minimum value of 0.6 and a maximum of 0.9. As discussed below, the battery pack is the crucial component of the whole system, and its cost, life and maintenance deeply influence the system's performance and reliability. Thus, by limiting the SOC we ensure a longer battery life and also longer time between system overhaul, decreasing all costs.

3. The Different System Configurations

Three basic configurations were initially considered, which differ from each other for the GT power management strategy:

- **GT-on/off (Configuration A):** The gas turbine either runs at idle or delivers full power. In this case, an extra requirement has been added to the design specifications: that the GT group is switched off when the train is in the station. Such choice is by no means necessary, but it improves the system *consumer friendliness*, reducing the visible emissions in a sensitive area (the railroad station) and also reducing the acoustic pollution there. When the turbine is "switched off", it really runs at idle, to avoid extreme cycling that is known to lower the total life of the thermal group. After the train leaves the station, the GT

group is ignited only when the SOC of the batteries becomes lower than a preset value (different for each optimal operational schedule). As shown in the flow charts of Figures 3 and 7, the turbine is then reset to idle as soon as the value of the SOC reaches the upper allowable limit. Additional minor adjustments are necessary to guarantee that the SOC is sufficiently higher than 0.6 when the train reaches its final destination (end of each single leg), so that the train can then be restarted in an all-electric mode:

- **GT-fixed (Configuration B):** The GT set runs at constant power throughout the mission. In this way we increase the life of the thermal group, thanks to a lower number of start-ups with respect to the previous case. On the other hand, the component subjected to the greater stress is now the battery package, because if the GT set is always ON the additional constraint of the bounding of the SOC level forces the battery to be charged and discharged continuously during the mission, reducing its operating life. Adopting the B configuration, the GT rated power corresponds to the average power of the mission, at the optimal (peak-efficiency) operating point, and the working mode is continuous, therefore the configuration B can be considered *a priori* the optimum solution from the fuel consumption point of view;

- **GT is following the load (Configuration C):** The main characteristic of the logic implemented in this configuration is that the GT supplies a constant power, at several power levels (80-110% of the rated GT power) defined according to the mission characteristics. These set points in general operate at lower-than-optimal efficiency, but it is now possible to avoid the ON/OFF working mode. In fact whenever the electric motor absorbs a larger power than that power produced by the turbine, the GT set begins to run at fixed point. The value of the electrical power is such as to guarantee a good value of the SOC during the mission. As noted above, this value is rigidly linked to the specific train and its specific mission, and it is no longer valid - for instance - for the same train on a different mission.

4. The Simulation Protocol

The simulation program is based on a simple input-output model for the energy fluxes through the system, and it was implemented as an aid for configuration design. As mentioned above, the GT set is switched on when the SOC is equal to or lower than a prefixed level, and it is set to idling or to a partial load mode when the SOC reaches the maximum allowable level. Naturally, in real operation, a manual override is always possible, but this was not considered in

our calculations. In hybrid-mode operation the batteries supply or absorb the difference between the net power demanded by the train and the net power supplied by the GT. The simulation quantitatively enforces such a protocol, calculating the instantaneous power demand as a function of the specified speed and acceleration (Capata and Sciubba 2002, Cioffarelli 2004).

The fuel consumption is computed on the basis of the specific "instantaneous" efficiency of the GT set and of its average power during a certain time interval. It was found that a Δt equal to 1 s reproduced accurately enough the power curve of the train: therefore, all simulations presented here are based on this timestep. The calculation of the electric motor power demand accounts for the power demand at the wheels and for both transmission and motor losses: in the acceleration phase or at constant speed, the electric motors provide traction energy, while in the braking phase a partial energy recovery is enforced to recharge the batteries. The instantaneous available power of the batteries, P_{ba} , thus depends on the SOC and on the energy requested by the electric motors. The batteries considered in this study are of the Pb-acid bipolar type, with a specific power P_{sp} of 150 W/kg and specific energy E_{sp} of 30Wh/kg: the power curve used in their simulation was based on data extracted from a previous independent experimental study conducted by the Italian National Energy Agency ENEA (TABLE I). The calculation of the battery charge and discharge process must take into account the necessity of an electronically enacted control of the current in and out of the battery, I_b : excessive values of I_b lead to rapid battery burn-out. Notice that, as specified in (Capata et al. 2003), it was assumed here that the GT could respond with negligible time lag to a change in the power demand. At the time this study was being conducted, no reliable data on other types of batteries could be found, and therefore no comparison of different electric storage devices was possible. It is likely, though, that the adoption of the Ni-Cd type which have higher power and energy densities with respect to the Pb-acid type, would lead to a lighter and more efficient power unit. As in a previous paper of this series (Capata et al. 2003) we used several mission profiles for the numerical comparison and for the program evaluation. Here, of the four railroad paths (Oslo-Skien, Skien-Oslo, Lillehammer-Asker, Asker-Lillehammer) for which complete mission data are available (Pede et al. 2003), we will consider only Lillehammer-Asker, which consists of approximately 1 hour of travel (about 45 km), and of the load demands shown in Figures 4 and 5.

Three different configurations were compared (TABLE II), in which the nominal

power of the gas turbine is substantially higher than the installed battery power (low degree of hybridization I_{hyb}). The aim of such a comparison is to accurately analyze the effects of three contrasting factors:

- 1) The expected increase in the fuel consumption, due to the fact that a more

powerful GT operates in off-design condition for the greater part of the mission;

- 2) The reduction of the weight and therefore of the cost of the electric storage with a reduced installed power;
- 3) A possible reduction of the specific mission consumption, obtained thanks to a better management of the power flows.

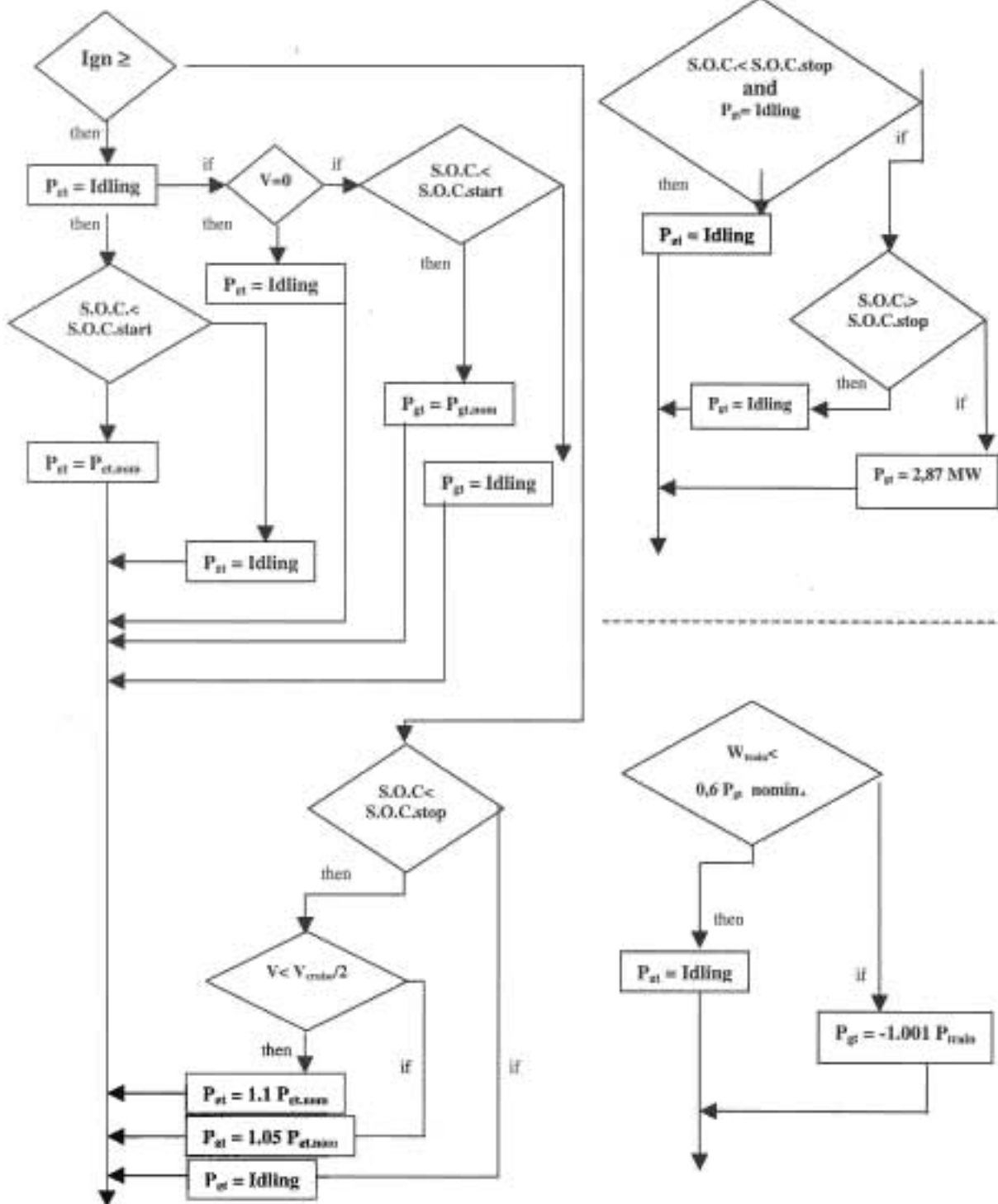


Figure 3. Flow chart of the logic of the three system configuration

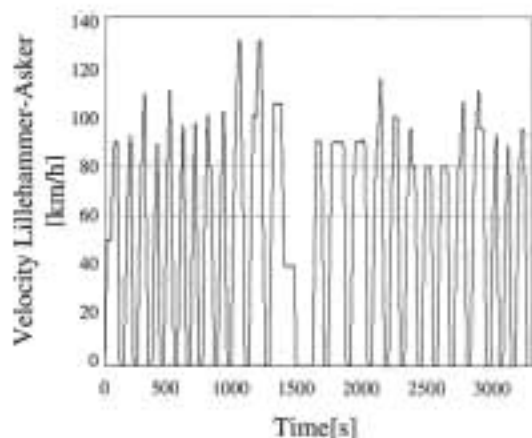


Figure 4. Diagram of the instantaneous speed

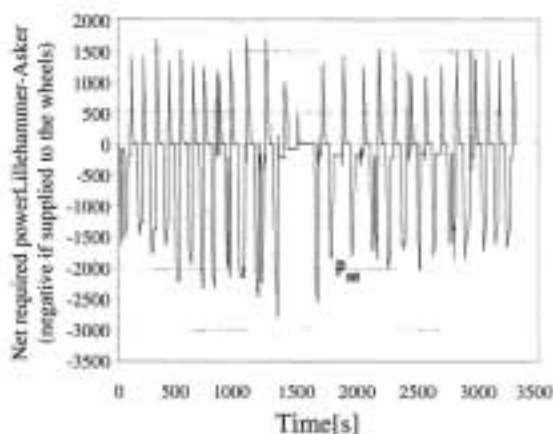


Figure 5. Diagram of the power demand for the Lillehammer-Asker train

Since the power-to-weight ratio is much higher for the GT than for the battery packages, three additional configurations were analysed, in which the installed GT power by far exceeded the average mission demand. These configurations (D, E, F) are likely to be affected by a higher fuel consumption per mission - because the GT works at part-load most of the time - but present the potential following advantages:

- The overall weight of the power unit is substantially lower than in configurations A, B and C, so that the train payload may be increased;
- The large available GT power surplus allows lowering of the variations of the battery SOC, and this leads to longer battery life;
- A smoothly varying battery SOC and an excess GT power are well suited for the installation of a properly sized set of ultra-condensers to buffer only the steepest peaks

in the power curve. UC would be substantially lighter and more efficient than batteries.

A last configuration (G) was simulated, in which the GT is chosen to be a commercially available machine, the Makila by Turbomeca. The reason for this further simulation was that, since a large set of operational data exist for the Makila, we could use this case as a validation both of our model and of our numerical procedure.

4.1 Imposed values

The values used in the simulation are reported in TABLE I:

TABLE I. CHARACTERISTIC PARAMETERS OF BATTERY MODULE

Module mass	$m_{mod} = 20 \text{ kg}$
Module voltage	$V_{mod} = 12 \text{ V}$
Cell voltage	$V_{cell} = 2 \text{ V}$
Specific power	$P_{sp} = 150 \text{ W/kg}$
Specific energy	$E_{sp} = 30 \text{ Wh/kg}$
GT switch-on setting	SOC < 60%
GT switch-off setting	SOC > 90%

TABLE II. FUEL CONSUMPTION OF THE CONFIGURATIONS STUDIED

	P_{GT} [kW]	P_{BAT} [kW]	Mode	c_{f^*} [g/kWh]
A	740	2060	on-off	239.8
B	350	2450	fixed	248.2
C	700	2100	load foll.	243.6
D	1500	1300	load foll.	235.9
E	1800	1000	load foll.	233.1
F	2000	800	load foll.	229.8

(* at rated power)

4.2 The balance equations

The formulae used for the calculation of the SOC, the fuel consumption, and the battery package weights are discussed in this section.

• Fuel consumption: Varying the GT net power, the fuel flow rate q depends linearly on the installed power P and on the off-design efficiency, as described by the following formula, where P is expressed in kW and q in kg/s:

$$q_{fd} = aP - b$$

where,

$$a = \frac{\eta_{nom}}{\eta_{od}} \cdot 3 \cdot 10^{-5}; \quad b = 5 \cdot 10^{-3} \cdot \frac{\eta_{nom}}{\eta_{od}}$$

thence,

$$c_x = q_{od} \cdot \frac{3600}{P_{ed}} \quad (4)$$

The fuel consumption of each one of the considered configurations has been calculated based on the specific consumption of the GT set and on its operational total "on" time during the mission (see Figure 6).

- SOC calculation:

$$SOC = SOC(i-1) + k_{bat} \cdot E_{bat} / P_{be} \quad (5)$$

where, SOC(i-1) is the SOC at previous time step, k_{bat} : energy penalty factor for battery charge/discharge, E_{bat} : battery instantaneous voltage, P_{be} : battery power required to absorb or provide the required energy.

- Battery package weight: The weight of the package is calculated as the ratio between the installed power and the specific one:

$$W = \frac{P}{P_{sp}} \quad (6)$$

As a first remark, we may notice that the specific consumptions (expressed in kg/mission in Figure 6) are lower for configurations D, E, F, contrary to what one would expect. The reason can be found by closer inspection of equation (4): the factor η_{nom}/η_{od} is - for the selected load-following set points - always very close to 1, and therefore the penalty in the instantaneous fuel consumption is relatively small and can be more than offset by the higher overall efficiency at which the battery pack is operated (smoother SOC curve).

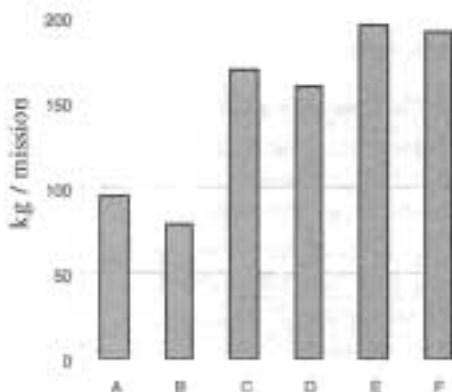


Figure 6. Comparison of fuel consumptions for the configurations studied

The procedure used can be summarized as follows. During the load following operation mode the GT is switched on if the SOC has already reached the minimal allowed level and the vehicle continues to demand energy; the rate at which the GT supplies power depends on the instantaneous difference between the demand, P_{net} , and the discharge capability of the battery pack P_{be} . In addition, the GT is switched back to idle whenever braking is on (and the battery is recharged by the recovered energy) or when the train comes to a stop. In this latter case, an additional control turns the GT on again if, for whatever reason, the battery SOC falls below the allowed minimum. The flow chart in Figure 7 displays the above logic.

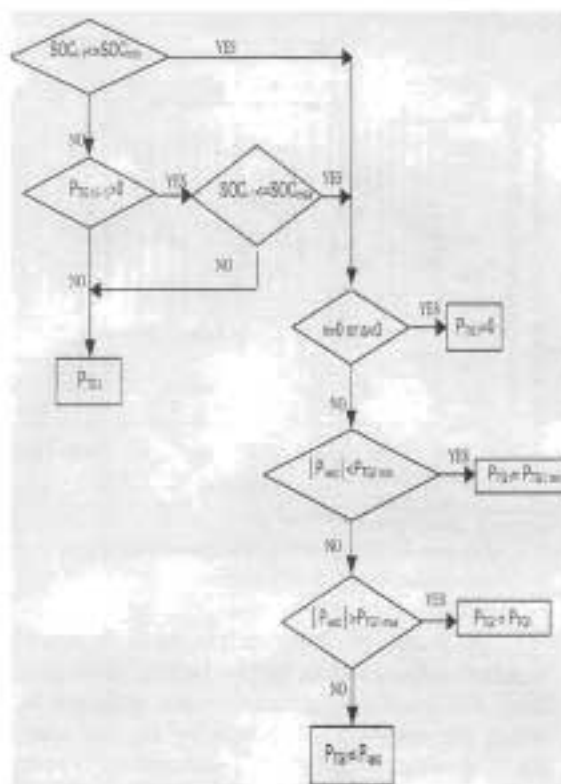


Figure 7. Flow chart of the logic

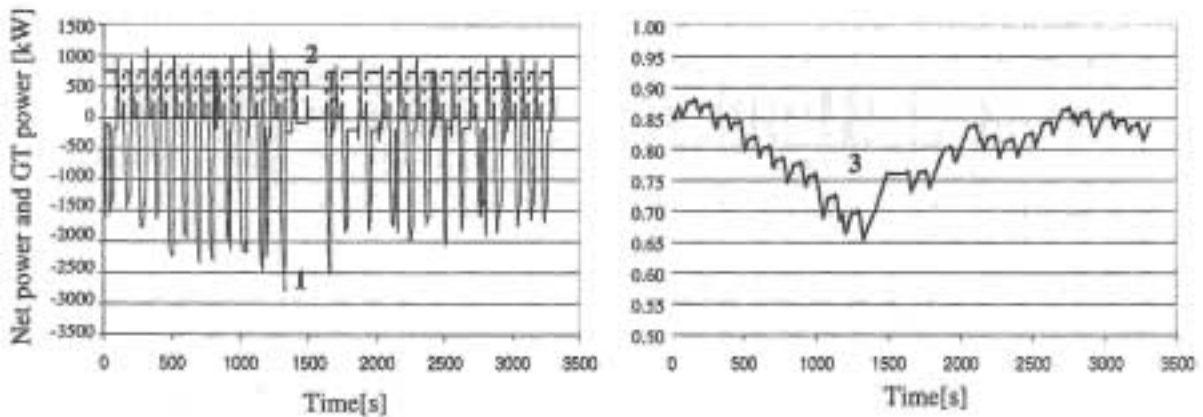
4.3 The results of the simulations

Figures 7 through 20 display the results of the simulations. For each configuration, three curves are reported:

- the net power demand, curve 1 (negative when absorbed by the wheels);
- the gross power delivered by the GT, curve 2;
- the battery state of charge, curve 3.

The battery power in and out is not shown here, but its value can be visually inferred by calculating the instantaneous difference between curves 1 and 2.

CONFIGURATION A



Figures 8, 9. Profiles of the net train power (1), GT power (2) and battery State of Charge (3), for $P_{gas\ turbine}=740\ kW$ and $P_{batteries}=2060\ kW$ (13,7 t) in On-Off mode

CONFIGURATION B

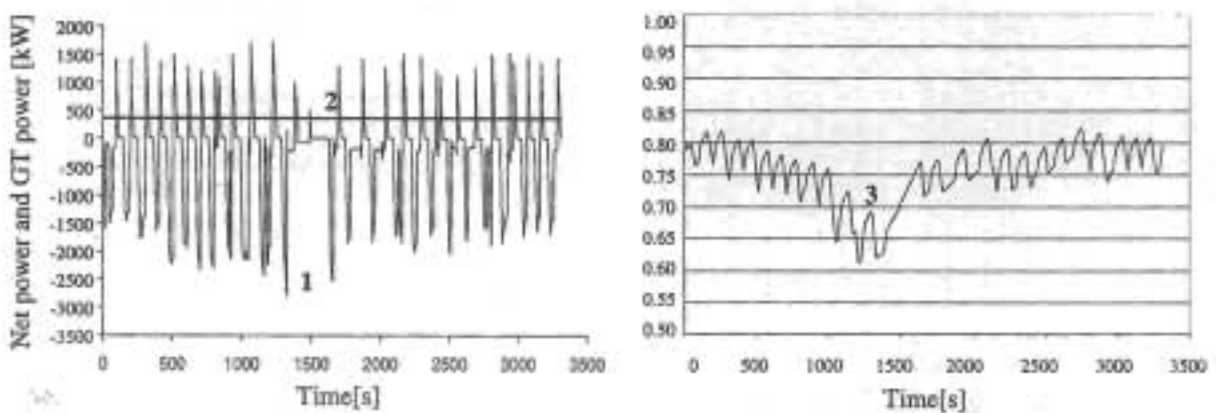
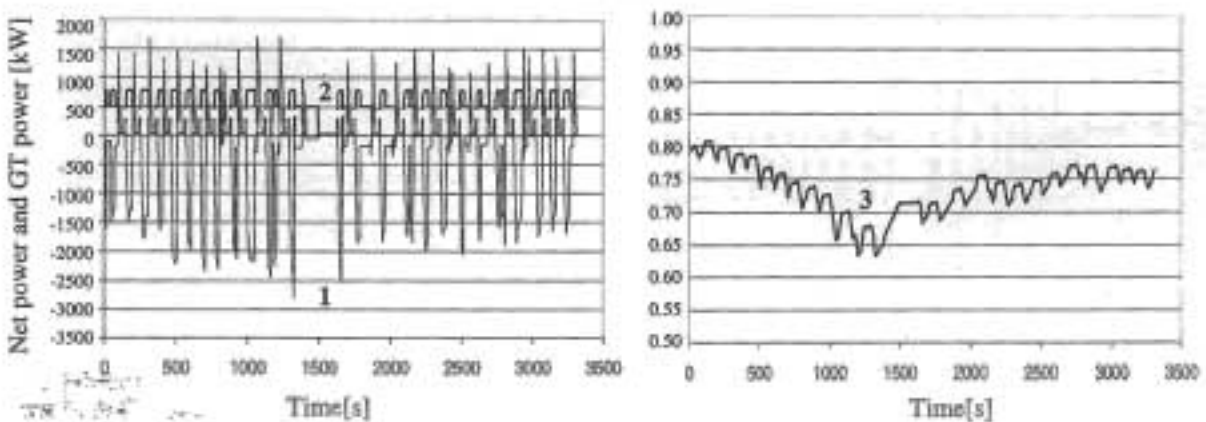


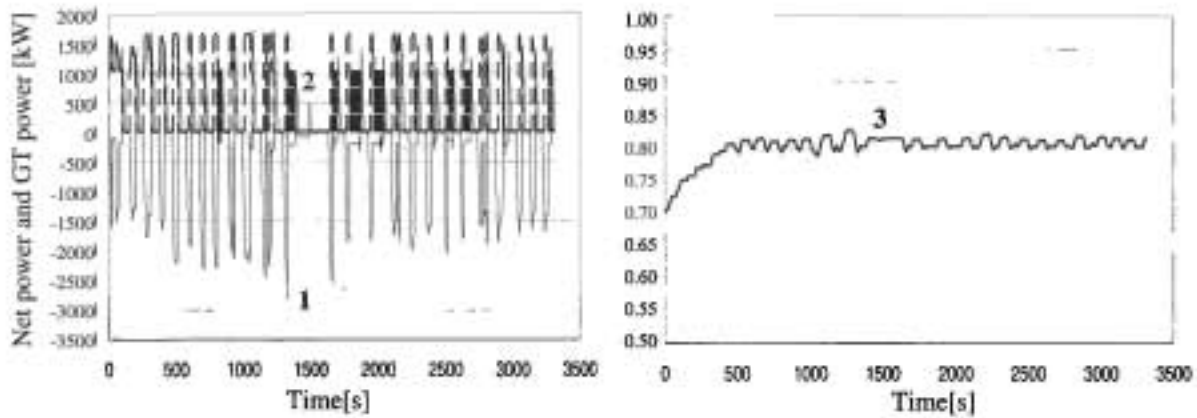
Figure 10, 11. Profiles of the net train power (1), GT power (2) and battery State of Charge (3), for a fixed $P_{gas\ turbine}=350\ kW$ and $P_{batteries}=2450\ kW$ (16,3 t)

CONFIGURATION C



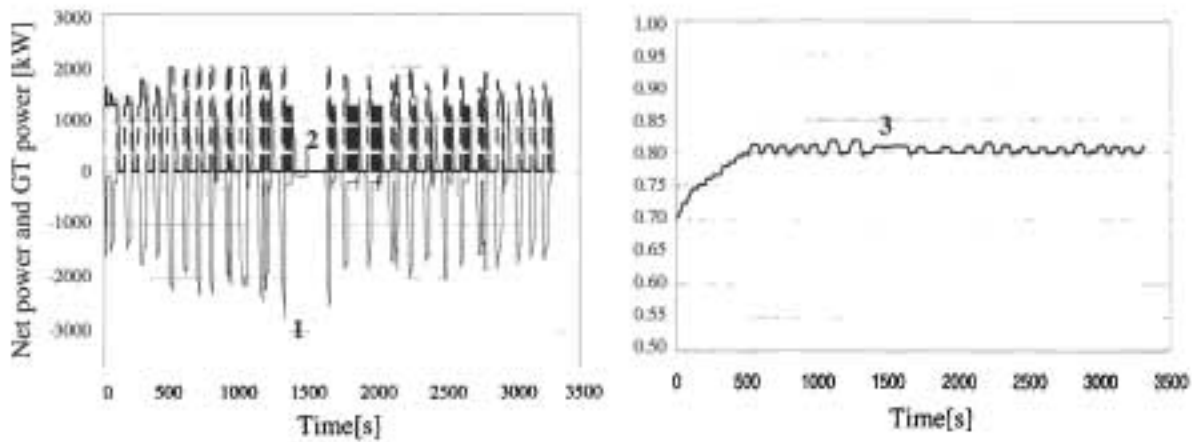
Figures 12, 13. Profiles of the net train power (1), GT power (2) and battery State of Charge (3), for a fixed $P_{gas\ turbine}=700\ kW$ and $P_{batteries}=2100\ kW$ (14 t)

CONFIGURATION D



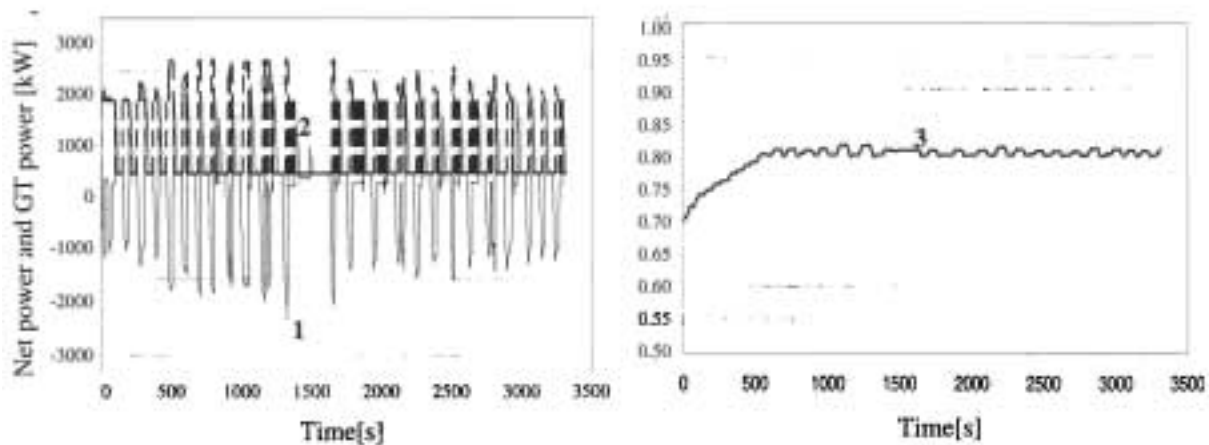
Figures 14, 15. Profiles of the net train power (1), GT power (2) and battery State of Charge (3), for $P_{gas\ turbine}=1500\text{ kW}$ and $P_{batteries}=1300\text{ kW}$ (10 t) in load-following mode

CONFIGURATION E



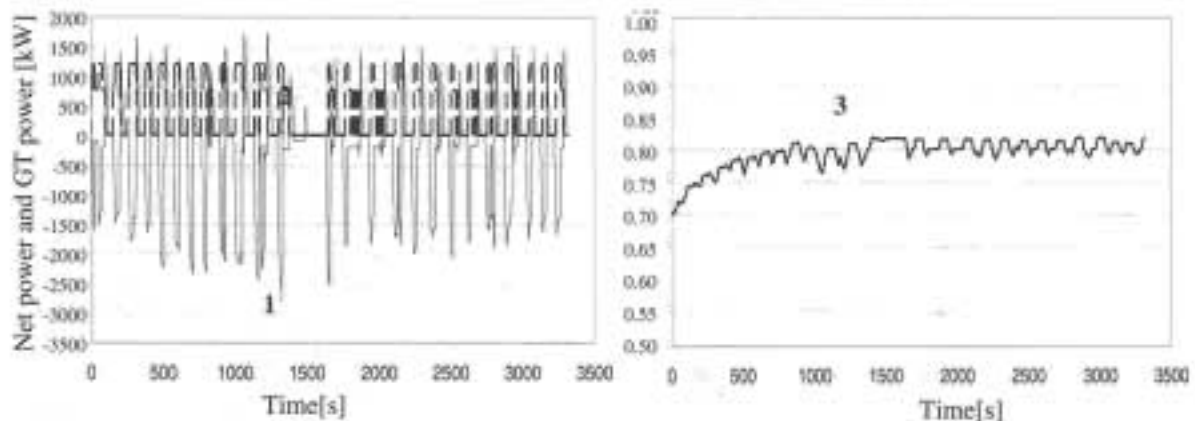
Figures 16, 17. Profiles of the net train power (1), GT power (2) and battery State of Charge (3), for $P_{gas\ turbine}=1800\text{ kW}$ and $P_{batteries}=1000\text{ kW}$ (8.7 t) in load-following mode

CONFIGURATION F



Figures 18, 19. Profiles of the net train power (1), GT power (2) and battery State of Charge (3), for $P_{gas\ turbine}=2000\text{ kW}$ and $P_{batteries}=800\text{ kW}$ (5.3 t) in load-following mode

CONFIGURATION G



Figures 20, 21. Profiles of the net train power (1), GT power (2) and battery State of Charge (3), for $P_{gas turbine}=1100$ kW and $P_{battery}=1700$ kW (11,3 t) in load-following mode

4.4 The validation on the Makila data

The simulation of the configuration F, the one with the Makila GT by Turbomeca, had the following goals:

- 1) To calibrate/validate our GT-cycle calculations by comparing the numerically derived cycle parameters with the available data;
- 2) To validate our first-order design procedure by comparing the overall dimensions and types of elementary components with those of the real machine;
- 3) To calibrate our weight and efficiency calculation procedures by directly comparing our results with the actual data.

TABLE III displays the assumptions made in the simulation, TABLE IV presents a direct comparison of some relevant quantities.

TABLE III. INPUT DESIGN DATA

Inlet pressure	$p_1 = 1.0 \cdot 10^5$ Pa
Air inlet temperature	$T_1 = 288$ K
Turbine Inlet Temperature	$T_3 = 1100$ K
Maximum shaft torque	$\tau = 4 \cdot 10^7$ N/m ²
Blade blockage coefficient	$\delta_b = 0.80$
Polytropic comp. efficiency	$\eta_{pc} = 0.8$
Polytropic turbine efficiency	$\eta_{pt} = 0.8$
Mechanical efficiency	$\eta_m = 0.85$
Electrical efficiency	$\eta_{el} = 0.9$
Natural gas LHV	$\Gamma_1 = 48000$ kJ/kg
Rotational speed	$n = 6350$ rpm
Maximum tip velocity	$u_{max} = 430$ m/s
Regeneration degree	$R = 0$
Net GT set power	$P_d = 1.1$ MW
Compression ratio	$\beta = 9.2$

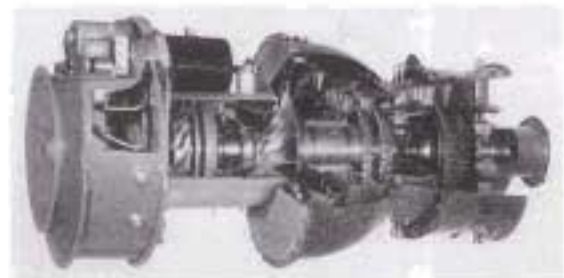


Figure 22. The Turbomeca MAKILA TI GT set

TABLE IV. RELEVANT VALUES FOR THE SIMULATION OF THE MAKILA GROUP

	P [MW]	n [rpm]	β	q [kg/s]	c_s [g/kWh]
simulation	1.1	6350	9.2	0.09	294
MAKILA	1.1	6350	9.2	0.089	291
	η_{GT} %	N_{comp}	N_{turb}	r_{inlet} [mm]	r_{max} [mm]
simulation	26	4	4	59.5	646
MAKILA	27	4	4	N.D.	N.D.

Notice that there is a good correspondence with the data of the MAKILA TI, with an overall efficiency of 27.4% (5% error) and a consumption of 291 g/kWh (1% error). The fuel consumption of 0.09 kg/s (1% error), assuming 15 daily hours of operation of the train at full power, requires a fuel tank containing approximately 5 tons of natural gas, which reduces to approximately 3.25 tons for an operation of approximately 10 hours. Assuming that the MAKILA is equipped with a control system that modulates the TIT (T_3) between 1100 K and 800 K, a simple zero-order procedure has been developed to determine the turbine characteristic curves and trace iso-

efficiency curves for the compressor and the turbine (Capata and Sciubba 2002, Capata et al. 2003, Cioffarelli 2004).

Figure 23 shows the variation of the GT available power as a function of T_3 . Assuming similarity with existing models, the maximum radial size of the GT set has been estimated about 1.3 times the maximum external radius of the rotating equipment, while the axial length is about 4 times the radial size. For a power range between 0.5 and 10 MW, data available from AnsaldoBreda provide an estimate of the GT installation cost equal to 0.45 \$/W.

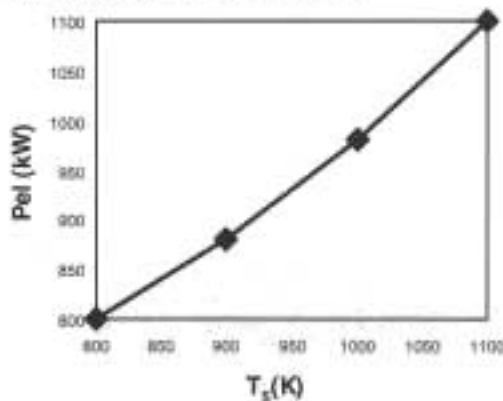


Figure 23. Variation of P_{el} as function of T_3

5. Cost Analysis

We assumed that the operational schedule of the TG-Hybrid train would consist of 10 missions per day, with an elapsed time per mission of 3400s and with 25 stops. Taking into consideration the expected technical lives of both the GT and the battery package, it is possible to compute the mission cost for every configuration studied. Assuming,

- Number of missions: $N_{miss} = 10/\text{day}$ Number of missions per year $A = 365$
- Mission elapsed time: $t_{miss} = 3400$ s
- GT life: $D_{GT} = 60.000$ h
- Number of possible missions for GT: $N_{GT} = D_{GT}/D_{mission} = 63530$
- GT installation cost: C_{GT} in TABLE III (Pede et al. 2002)
- Scheduled maintenance every 4000 operational hours (15 total): cost $K_1 = 2\% C_{GT}$ (Pede et al. 2002)
- System overhaul every 20000 operational hours (3 total): cost $K_2 = 10\% C_{GT}$ (Pede et al. 2002)
- Maintenance total cost: $C_{maint} = K_1 + K_2$
- Battery package installation cost: $C_{BT} = 10$ (\$/kg) (Pede et al. 2002)
- Average supplied battery power during a

mission: $P_{average}$ batteries mass M_{BT}

- Average specific battery power during a mission: $P_{sp,average} = P_{average}/M_{BT}$ [W/kg]
- Useful battery mileage: $p = 69122 e^{(-0.049 P_{sp,average})}$ [km] (Pede et al. 2002)
- Battery-powered kilometers per mission: Z (computed)
- Number of missions for a single battery package: $N_{BT} = p/Z$
- Fuel cost: $c_{fuel} = 0.5$ \$/kg (Pede et al. 2002)
- Total labor annual cost: $C_{lab} = \$30.000/\text{year}/\text{person}$

The mission cost can be computed, in \$ 2003:

$$C_{mission} = C_{fuel,y} + C_{GT,y} + C_{BT,y} + C_{maint,y} + C_{labory,y}$$

The calculations provide the following results for the weights and the installation costs of the hybrid system*:

To calculate the annual operational cost, a standard cost-actualization was performed, assuming the economic life of the GT equal to 15 years, a fixed interest rate of 5%, zero residual value, and all of the batteries purchased at time $t = 0$. We obtain:

$$R = [(1+i)^{15} - 1] / [(1+i)^{15} - 1] = 0.096$$

$$C_{GT,y} = R \cdot C_{GT}$$

$$C_{BT,y} = R \cdot C_{BT} \cdot N_{BT} / N_{BT,y}$$

$$C_{maint} = 2\% C_{GT,y} + 10\% C_{GT,y}$$

$$C_{lab,y} = 30.000 \text{ $/year}$$

$$C_{fuel,y} = A \cdot C_{fuel,mission} = A \cdot c_{fuel} \cdot q$$

From a comparison of TABLES II, V and VI, we can draw the conclusion that, under the present assumptions and mission specifications, the optimal configuration is B ($P_{GT} = 350$ kW, $P_{te} = 2450$ kW), which offers (TABLES V and VI) the lowest fuel consumption (79.6 kg/mission which correspond to 8.3 g/h/km or 8.8 g/passanger/km*), the lowest initial cost (\$338,000), and, in spite of its higher maintenance and battery replacement costs, the lowest overall yearly costs (399,233 \$/yr).

Notice, though, that configurations D, E and F are suitable for the adoption of ultra-condensers (Figures 14-19), while configuration B is not (Figures 10 and 11).

* No explicit calculation has been carried out to take into account the weight of the fuel tanks. All data presented in this paper assume CH_4 is used as fuel.

* Calculated assuming an average occupancy of 200 passengers/mission

TABLE V. GT SET AND BATTERY PACK COST AND WEIGHT FOR THE STUDIED CONFIGURATIONS

	Batt. Weight [t]	Batt. Inst. Power [MW]	Batt. Average Supplied Specific Power [W/kg]	Batt Total Mil. [km]	Batt Total # Miss. [N _{miss}]	GT Install Power [kW]
A	13.7	2.06	33.3	13462	606	740
B	16.3	2.45	24.4	20912	1349	350
C	14	2.1	25.6	19773	1167	700
D	8.7	1.3	17.1	29780	1188	1500
E	10	1	61.5	3391	139	1800
F	5.3	0.8	80.2	1356	54	2000
G	11.3	1.7	31.8	14531	632	1100
	GT M [kg]	Alt. M [t]	Fuel Cons. F [kg/miss]	Initial cost GT [\$x 1000]	Cost Batt. [\$x 1000]	Total initial cost [\$x 1000]
A	370	1.4	96	370	137	507
B	175	0.7	79.6	175	163	338
C	350	1.4	170	350	140	490
D	750	3	159.7	750	87	837
E	900	3.6	196	900	100	1000
F	1000	4	192	1000	53	1053
G	550	2.2	190	550	113	663

TABLE VI. OPERATIONAL COSTS OF THE SEVEN STUDIED CONFIGURATIONS

	C_{GTa} \$/year	C_{Btts} \$/cycle	C_{Btts} \$/year	C_{miss} \$/year
A	35520	13152	79196	16440
B	16800	15648	42333	19560
C	33600	13440	42026	16800
D	72000	8532	25652	10440
E	86400	6432	167737	8040
F	96000	5088	340864	6360
G	52800	10848	62644	13560
	$C_{lab a}$ \$/year	$C_{fuel a}$ \$/year	Annual cost \$/year	
A	30000	351677	512833	
B	30000	290540	399233	
C	30000	623055	745481	
D	30000	671600	809692	
E	30000	715400	1007578	
F	30000	700800	1174024	
G	30000	693500	852504	

TABLE VII. COMPARISON OF THE SPECIFIC OUTPUT CHARACTERISTIC OF BATTERIES AND ULTRA-CONDENSERS

	Power [kW/kg]	Energy [kWh/kg]
BATTERIES	0.15	0.035
ULTRA-CONDENSER	3.7	0.002

6. Conclusions

A series of numerical simulations of the energy flows through the power section of an EMU-train equipped with a novel GT-hybrid propulsion system were conducted. An all-electric version of the train, with a total weight of about 197 tons, operates within the Norwegian railroad system. The results indicate that the design choice of the relative power mix (ratio between the GT power and the total installed power, also called degree of hybridization) has a direct influence not only on the power response ("driveability") of the system, but also on the life of the batteries, the efficiency of the gas turbine, the overall dimensions of the system and the mission cost.

We performed a preliminary comparison of different configurations, with installed GT powers of 350, 700, 740, 1500, 1800 and 2000 kW respectively, varying for each one the compression ratio between 3 and 30 in order to find an optimal value. To validate our computations, a separate run of the procedure was implemented under a special set of design specifications, so that they would result in the choice of an existing GT-set, whose performance data could then be used for validation purposes.

Under our assumptions the "optimal" configurations is B, for fuel consumption, initial cost and overall yearly cost.

In perspective, one should remark that configuration D ($P_{GT} = 1500$ kW, $P_B = 1300$ kW) displays an SOC behavior along the prescribed mission that makes it a suitable candidate for the adoption of ultra-condensers, which offer substantial advantages in terms of weight, cost and maintenance with respect to the Pb-acid batteries considered here.

The results indicate that besides studying the possibility of installing batteries with greater power and specific energy than the Pb-acid considered here, it would be advisable to investigate the possibility of using a double electric storage (matching batteries and ultracondensers), and to perform a complete technical-economic analysis of a hybrid solution with more than one type of accumulation system (for instance, flywheel + battery).

The low energetic density of the currently available batteries limits the feasibility of hybrid vehicles operating in an "only-electric" mode. If only marginal improvements in the performance and the cost per mission are attained, markets could only in fact react positively to the introduction of hybrid trains.

The possibility of using a more accurate (1) management system and a more efficient electrical storage system will make the hybrid optimum competitors, in terms of cost and performance, of current vehicles, but the actual production cost of hybrid vehicles can really be determined only when production reaches industrial scale. Fiscal and governmental incentives could undoubtedly encourage the commercialization of such vehicles.

Nomenclature

b	width [m]
C	cost [S]
c	fuel consumption [g/kWh]
c_d	aerodynamic drag coefficient
D	technical life [yrs]
E	energy [kJ]
f	wheel-rail/rack friction coefficient
h	height [m]
i	current [A]
r	interest rate
k	energy penalty factor for battery charge/discharge
L	useful mileage [km]
m	mass [kg]
N	number of missions
n	rpm
P	power [W]
p	pressure [bar]
q	flow rate [kg/s]
r	rolling radius of the train wheels [m]
R	reimbursement rate [S/yrs]
R_p	degree of regeneration
S.O.C.	battery State Of Charge
T	temperature [K]
t	time [s]
TIT	Turbine Inlet Temperature [K]
U_{max}	impeller maximum tip velocity [m/s]
V	voltage [V]
α	slope of the track [°]
β	compression ratio
Γ	low heating value units [kJ/(kg°C)]
δ	blade blockage coefficient
η	efficiency
τ	torque [Nm]

Acronyms

AC/DC	inverter
B	battery
BC	battery charger
C	compressor
CC	combustion chamber
G	electrical generator

IGV	Inlet Guide Vane
M	electric motor
RE	regenerator
VMI	vehicle management unit
VIGV	Variable Inlet Guide Vane

Subscripts

batt	battery package
br	battery module
cell	cell
el	electrical
fuel	fuel
gen	electrical generator
labor	labor
m	mechanical
maint	maintenance
miss	mission
mod	module
nom	nominal
od	off design
pc	polytropic compressor
pt	polytropic turbine
sp	specific
train	train
transm	transmission
y	year

References

- Ansaldovereda, 2001 P/N - AA016LG *Envy for NSB*
- Cipala R, Scubba E., 2002 *Simulation and Experimental Results of a 15 kW Hydrogen Turbogas for a Series Hybrid Vehicle*. Proc 14SDA2002 6th Biennial Conf on Eng Sys Design and Analysis, Istanbul Turkey.
- Cipala R, et al., 2004 *A Gas Turbine-Based Hybrid Vehicle - Part II: technological and configuration issues* *ENER* 2004 July, V 125 p 777-782
- Ciolfarelli E. 2004 *Modeling of a Gas Turbine driven hybrid propulsion system for a commercial passenger car* - Ph.D Thesis, U of Roma I
- EPCOS AG www.epcos.com
- Pedre G, et al., 2003, *High power lead-acid battery for heavy-duty HEV on the road and laboratory performance and reliability assessment*, - SAE World Cong "Advanced Hybrid Vehicles Powertrains 2003", SAE SP-1750, Detroit
- Pedre G, et al., 2007- *Hybrid storage system an optimization case* SAE paper 2002-01-1914, "Power", Special Issue, 2000
- Rautenberg M., Maliniche M., 1985 *On Turbochargers with Variable Geometry*, ASME paper 85-GT-149
- Sovran G., Hucko W.H., 1993 *Aerodynamics of road vehicles*, Ann. Rev. Fl Mech